Pressure-Time History of Pylon Wake on a Pusher Propeller in Flight

Saeed Farokhi*
University of Kansas, Lawrence, Kansas 66045

Miniature, high-frequency, pressure transducers were mounted on a pusher propeller at 75 and 90% radii. Time history of fluctuating surface pressure over 700 propeller revolutions and 26 flight conditions reveals intriguing phenomena. The anticipated pylon wake signature manifests itself as a negative pressure pulse over extended portions of the propeller suction surface. The phenomenon further develops into a primarily random turbulence signature at 80% propeller chord and interestingly may re-evolve as a coherent wake signature further downstream, say at 90% chord. A new type of periodic disturbance of long-time scale, compared to propeller period of revolution, is discovered at positions beyond 0.6 chord on the propeller suction surface in the transonic regime. These and other peculiar propeller-surface events recorded by the transducers are highlighted, and some plausible explanations are offered.

Nomenclature

C_{pylon} = pylon chord length, 59.9 in.
c = propeller chord length, in.
D = propeller diameter, 100 in.
J = propeller advance ratio, $\equiv V/nD$
M_r = helical Mach number
n = propeller shaft frequency, cps
P_{t_∞} = flight total pressure, psia
$P_{t_{\text{wake}}}$ = total pressure in the pylon wake, psia
T_{prop} = period of propeller revolution, s
x = coordinate along propeller chord, in.
y = pylon wake coordinate normal to pylon chord, in.
β_{prop} = propeller pitch angle measured with respect to plane of rotation, deg
β_{75R} = helical flow angle at 75% radius measured with respect to propeller plane of rotation, deg
β_{90R} = same as β_{75R}, but at 90% propeller radius, deg
$\Delta\alpha$ = propeller angle of attack, deg (Fig. 13)
$\Delta\beta$ $\equiv \beta_{\text{prop}} - \beta_{75R}$ or $\beta_{\text{prop}} - \beta_{90R}$, deg
ω = propeller shaft rotational speed, rpm

Introduction

THE problem of pusher propeller noise and unsteady aerodynamics can best be studied by directly investigating fluctuating propeller blade surface pressure. This problem is even more challenging if the data are to be acquired in flight. Wind-tunnel experiments to simulate flight conditions, usually on a scaled model, produce well-conditioned test environments but can hardly simulate the real flight situation. Sources of unsteadiness for a subsonic pusher propeller are 1) angle of attack or sideslip, i.e., flow angularity with respect to the propeller plane, 2) upstream wing or pylon wake interaction, 3) flow turbulence and gust, and 4) engine exhaust stack interaction with the propeller. From these, flow angularity causes cyclic loading with the azimuthal wave number of one. However, at higher subsonic speeds, i.e., with helical Mach numbers in the transonic range, the sinusoidal surface pressure response to angle of attack is distorted by the appearance of shocks, boundary-layer separation, etc. This point will be further discussed in the paper. Upstream pylon or wing-wake interaction is the source of a highly localized (in azimuthal plane) one or two excitations per revolution, typically with higher harmonic amplitudes one or more orders of magnitude smaller. Flow turbulence and gust produce broadband response by the propeller blades. Finally, the jet(s) emerging from the engine nozzle(s) produce one or two excitations per revolution for the pusher propellers, typically near the root. For advanced transonic propellers, the appearance and oscillation of impinging shocks on the blade turbulent boundary layer, because of the previously mentioned sources of unsteadiness, introduce a new source for noise radiation. Unsteady, turbulent, boundary-layer separation and reattachment, in response to an impinging, oscillating shock, represents the new noise source. Besides the broadband turbulence noise radiation from the boundary layer, the phenome-

Received May 11, 1989; presented as Paper 89-2052 at the AIAA/AHS/ASEE/Aircraft Design and Operations Meeting, Seattle, WA, July 31, 1989; revision received Sept. 17, 1989.

*Associate Professor, Aerospace Engineering Department. Member AIAA.

Table 1 Summary of flight conditions

Condition	Altitude, ft	Indicated airspeed, knots	rpm	Flap, deg
1	35,000	120	2000	0
2	35,000	120	1700	0
3	35,000	150	2000	0
4	35,000	150	1700	0
5	15,000	210	2000	0
6	15,000	210	1700	0
7	15,000	180	1700	0
8	15,000	180	2000	0
9	15,000	150	2000	0
10	15,000	150	1700	0
11	15,000	120	1700	0
12	15,000	120	2000	0
13	15,000	200	2000	20
14	15,000	200	1700	20
15	15,000	180	1700	20
16	15,000	180	2000	20
17	15,000	150	2000	20
18	15,000	150	1700	20
19	15,000	120	1700	20
20	15,000	120	2000	20
21	15,000	175	2000	35
22	15,000	175	1700	35
23	15,000	150	1700	35
24	15,000	150	2000	35
25	15,000	120	2000	35
26	15,000	120	1700	35

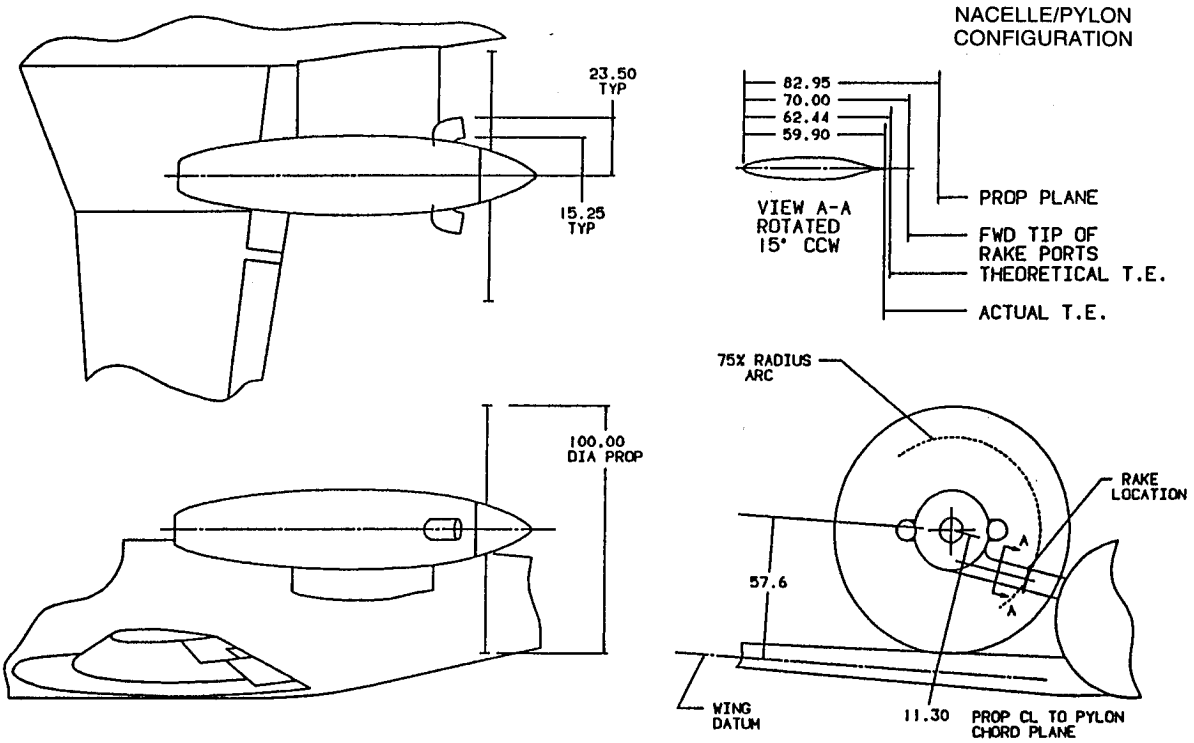

Fig. 1 Flight configuration of the advanced turboprop test-bed aircraft (all dimensions in inches).

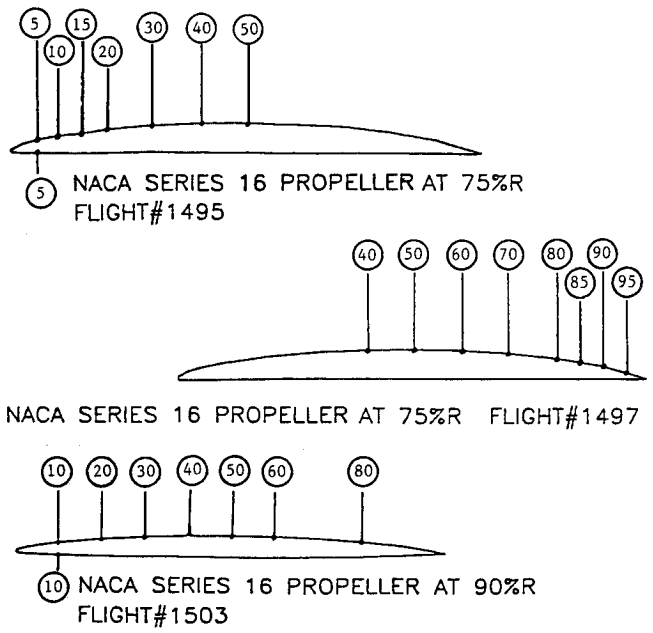

Fig. 2 Transducer locations on the instrumented propeller blade at 75 and 90% radii (in each flight, the ac signals from eight transducers were recorded).

non exhibits the characteristic frequency of the oscillating shock.

In the present study, a test-bed pusher propeller aircraft with a pylon-mounted nacelle was flown in 26 flight conditions covering the range of aircraft speed, shaft rpm, altitude, and wing-flap setting. Table 1 shows these flight conditions. The test-bed aircraft flight configuration is shown in Fig. 1. Interesting features of the pressure-time history of the blade-surface transducers as a result of pylon wake encounter as well as other peculiar phenomena are presented and discussed.

Instrumentation

A propeller blade was instrumented at 75 and 90% radii with 22 surface-mounted, high-frequency miniature pressure transducers. The two exhaust stacks discharged engine products of combustion near the propeller root; i.e., the jet centerline is at 0.38 blade radius. The location of the pressure transducers is shown in Fig. 2. The numbers in circles represent percent chord position. Fourteen transducers were mounted at the 75% radius and eight at the 90% section. Because of recording channel limitations (of eight), two flights were necessary to complete the 14 blade-mounted transducers (BMTs) at the 75% radius. The 40 and 50% chord BMTs were repeated in both flights (at the 75% radius) to insure repeatability of the experiments. Figure 3 serves as the definition sketch for the propeller angular position and reference plane. The instrumented propeller passing was sensed by a magnetic pickup, which registered a peeper signal on a magnetic tape. Since the period of oscillation is equal to the inverse of the frequency of oscillation, a transducer with a natural frequency of 230 kHz can resolve a phenomenon of time scale equal to 4 μs. Hence the propeller of 33 Hz frequency (i.e., 2000 rpm) with a period of revolution equal to 30 ms has a spatial resolution of nearly 7500 points (or oscillations) in one cycle. If the wake encounter by the instrumented propeller is limited to, say, 10 deg in the azimuthal direction, then the wake signature on the propeller is resolved by over 200 oscillations or points. This provides more than adequate information on the propeller-wake encounter. The digitizing rate of the analog data (performed at NASA Langley) was set at 10 kHz, providing nearly 300 data points per revolution. The telemetry system response was 20 kHz.

An optimum method of BMT mounting on the propeller blade surface is described by Heidelberg and Clark.[4] Their method requires the transducer to be mounted at the bottom of a cavity below the surface. However, for the in-flight measurement of blade-surface pressures, it was decided to vacuum seal the transducers directly on the blade. The advantage of this technique is in maintaining the structural integrity of the propeller blades. The disadvantage is due to the transducer plate protrusion of 0.001 in. into the flow, followed by

the actual transducer thickness of 0.015 in., which primarily alters the local surface curvature on the blade. The effect of modified surface curvature is believed to manifest itself as an offset on the transducer dc value and not significantly influence the dynamic signal representing local unsteady pressure. As will be discussed later, the surface mounting of the BMTs on the instrumented propeller did not trigger early transition in the boundary layers either. This fact was evidenced from pressure-time history plots of near-leading-edge BMTs.

The pylon wake was measured by a rake normal to pylon chord at a location corresponding to 75% propeller radius. All of the 26 flight conditions were measured in one flight, designated as flight 1498. The close coupling of the wing flap and the pylon caused a major shift in the wake centerline. This is discussed further in the next section. With the fixed rake position and a shifting wake (with the flight condition), the minimum velocity point did not register by a rake port for all conditions.

References 1, 2, and 4 describe the details of telemetry system, data acquisition, and installation of miniature BMTs.

Pylon Wake Measurements

Total pressure deficit in the pylon wake was measured via a fixed rake positioned at $0.17C$ location (where C is the pylon chord) downstream of the pylon trailing edge. The wake coordinate y is positive downward and normal to the pylon chord. The scanivalve recording was averaged over 12 sets of data taken in flight (i.e., nearly 30 s of data acquisition per flight condition) to arrive at an average wake profile, statistically representative of the mean flow in the pylon wake. Figure 4 represents an ensemble of the wake total pressure deficit profiles over all of the flight conditions. The wake centerline is shifted below the plane of the pylon chord in flight conditions where positive flap was applied. For example, in flight conditions 21 and 22, with flap position of 35 deg, the pylon wake centerline is shown in Fig. 4 to shift downward by nearly 2 in., i.e., $Y/C \approx 0.03$. The low deficit wakes correspond to the low speed flights. Propeller rotational speed (i.e., 1700 and 2000 rpm) had no measurable effect on the average wake deficit flow. This is shown by pairing of wake profiles in Fig. 4 in groups of two, corresponding to two propeller angular velocities. It may also be noted (from Fig. 4) that some of the wake profiles could not be entirely captured by the rake for some flap positions. The Reynolds number based on the 5-ft pylon chord for various flight conditions varied between $5\text{–}10 \times 10^6$. Hence, propeller/wake interaction took place with a turbulent momentum-deficit shear layer, which clearly made its mark on the pressure traces.

Pressure-Time History

In this section, due to space limitations, we propose to examine a few interesting BMT responses at a few flight conditions.

75% Propeller Radius

At 75% propeller radius, 14 BMTs were installed: one on the pressure surface at $x/c = 0.05$; the remaining 13 on the suction surface at $x/c = 0.05, 0.10, 0.15, 0.20, 0.30, 0.40, 0.5, 0.6, 0.7, 0.8, 0.85, 0.9$, and 0.95, as shown in Fig. 2. Flight condition 11 is chosen to represent the basis for further discussions. It represents the lowest helical Mach number of $M_r = 0.585$ and no flap deflection. We further note that the propeller was lightly loaded as $\Delta\beta = 0.9$ deg. The minimum velocity point in the pylon wake introduced an additional loading of 8.9 deg (or a total $\Delta\beta_{max}$ of 9.8 deg) to the propeller. The pressure-time histories of 12 BMTs over 100 revolutions are shown in Figs. 5a–5l for this flight condition. The other two pressure transducers, namely the 10 and 95% chord BMTs, were either saturated, as for the 10%, or left out to save space. The random signature at 0.95 chord BMT was very similar to the 0.90-chord pressure-time history, which is shown in Fig. 5l.

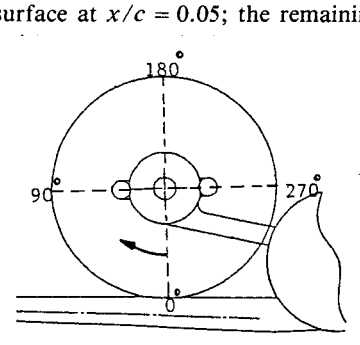

Fig. 3 Definition sketch of the propeller angular position (rear view).

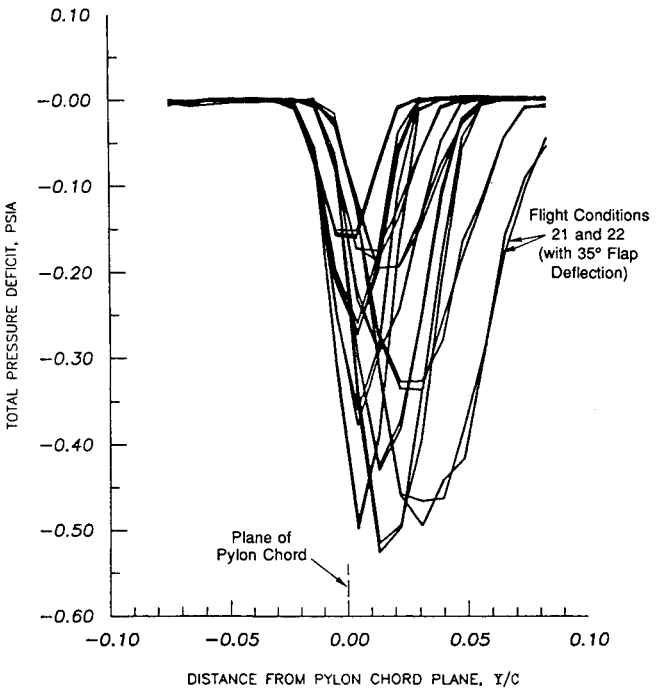

Fig. 4 Pylon total pressure wake profile, all conditions.

The response of the pressure-surface BMT in flight condition 11 to the incoming flow angularity and the pylon wake for 100 revolutions is shown in Fig. 5a. The aircraft angles of attack (pitch, yaw, and roll) manifest themselves in a one-cycle pressure wave trace in Fig. 5a. If the reader has difficulty discerning this point from Fig. 5, it is primarily due to the vertical scale compression to fit 100 waveforms on one graph. To illustrate the point further, average waveforms (over 100 revolutions) for the 5% pressure and suction surface BMTs are shown in Figs. 6a and 6b, respectively. The one-cycle wave due to flow angularity shows nearly the same amplitude as that of wake encounter near the 300 deg angular position. The pylon wake signature on the propeller is clearly visible as a negative pressure pulse for the 5 and 15% suction surface BMTs in Figs. 5b and 5c, respectively. The amplitude of the suction pulse is diminished further downstream, as shown in Figs. 5d–5i. At 80% chord, i.e., Fig. 5j, pressure-time history depicts a random turbulence signature, which masks any coherent wake interaction structure near the 300 deg position. Figures 5k and 5l show essentially pressure fluctuations in a turbulent boundary layer communicated to the surface and nearly unaffected by the upstream wake. The average waveforms over 100 revolutions, however, for 85 and 90% chord BMTs, do show a very small "blip" near the 300 deg position in Figs. 5k and 5l. With the benefit of hindsight, the overall surface pressure behavior at flight condition 11, which corresponds to a below-critical (helical) Mach number and small

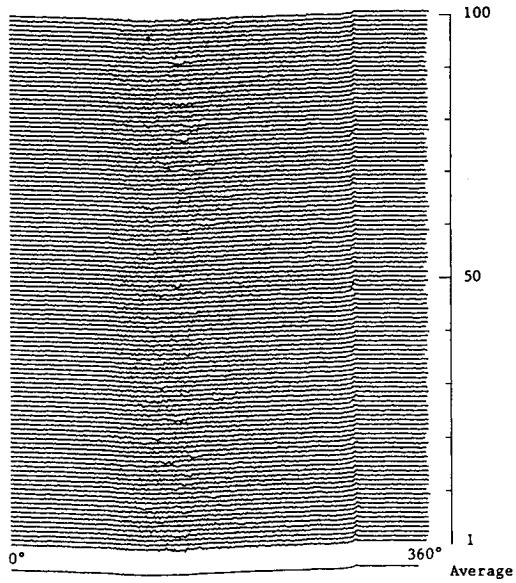

a) Transducer No. 75R05L

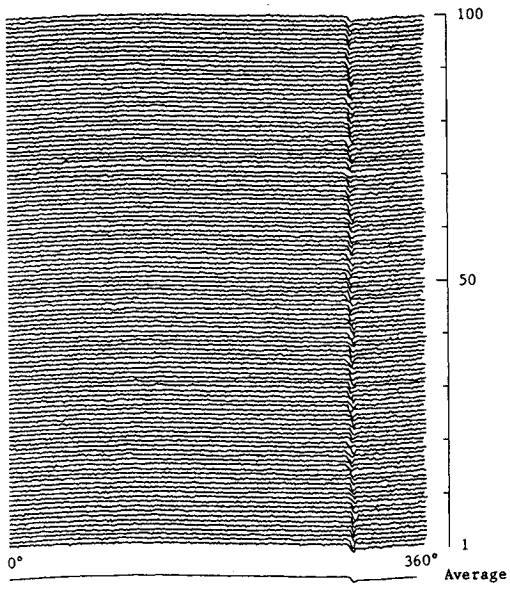

b) Transducer No. 75R05U

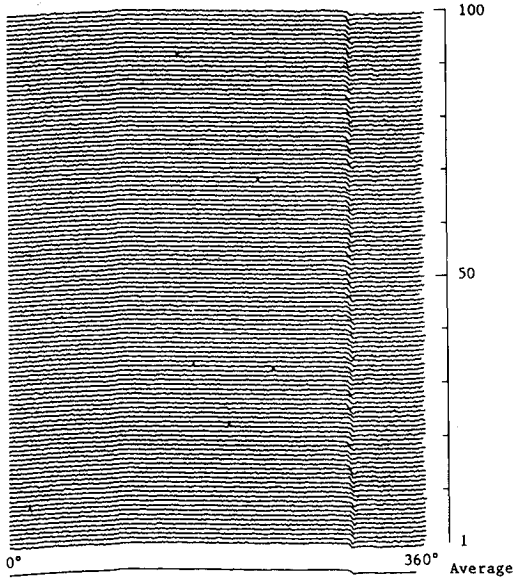

c) Transducer No. 75R15U

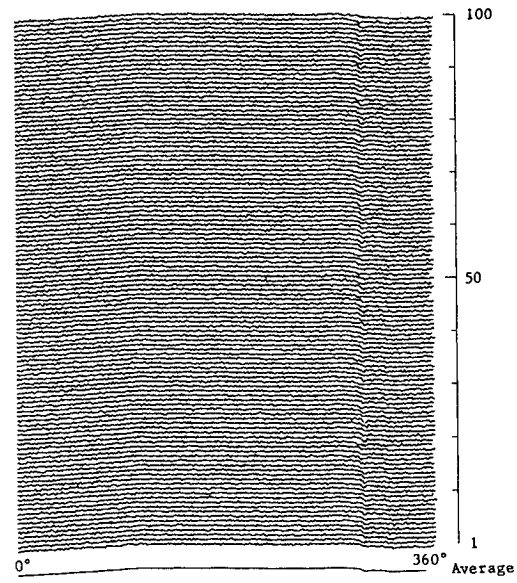

d) Transducer No. 75R20U

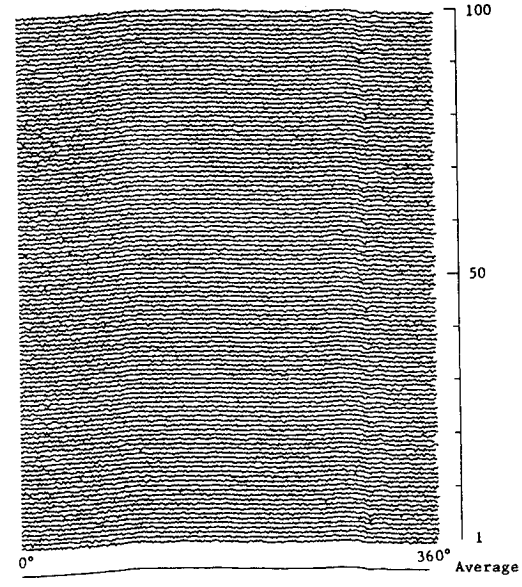

e) Transducer No. 75R30U

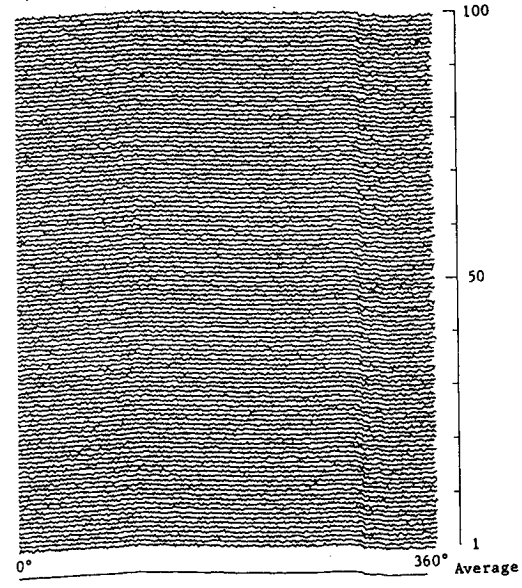

f) Transducer No. 75R40U

Fig. 5 Pressure-time history over 100 revolutions at 75% propeller radius at flight condition 11; helical Mach number at 0.75R, $M_r = 0.585$, advance ratio $J = 1.13$, $\beta_{75R} = 25.7$ deg, and $\beta_{\text{prop}} = 26.6$ deg.

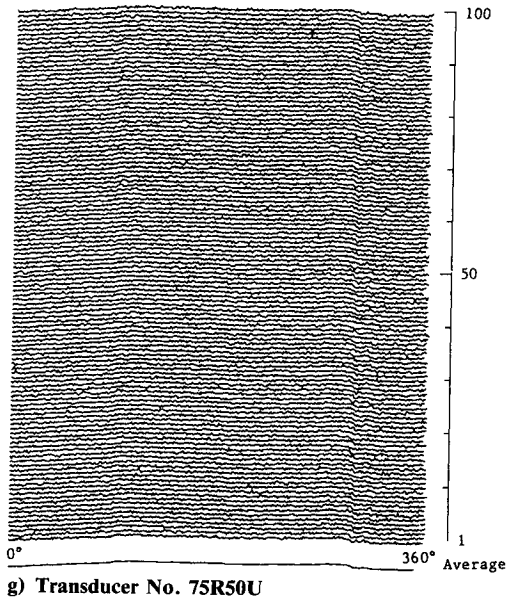

g) Transducer No. 75R50U

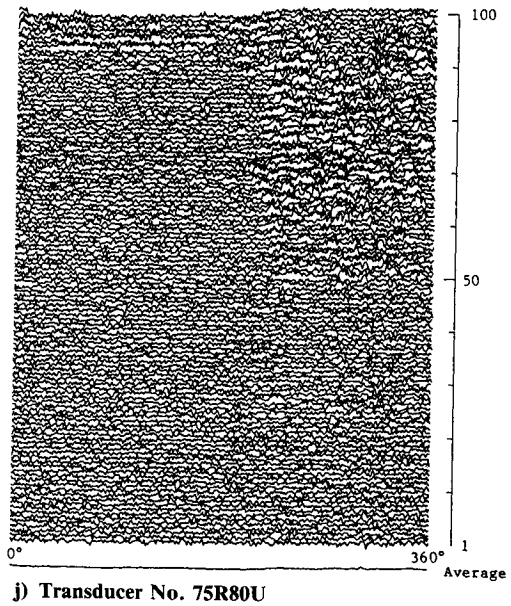

j) Transducer No. 75R80U

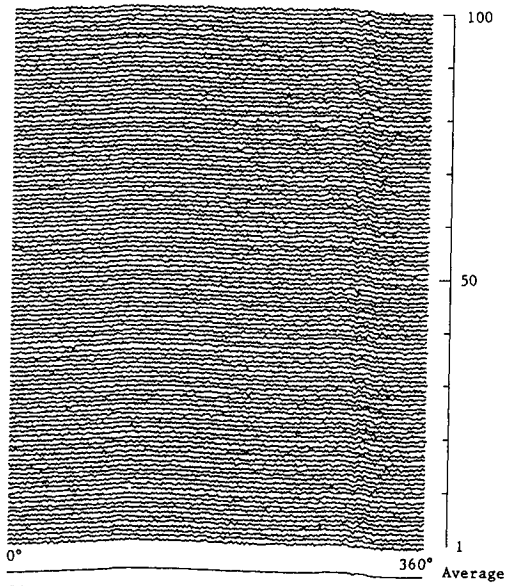

h) Transducer No. 75R60U

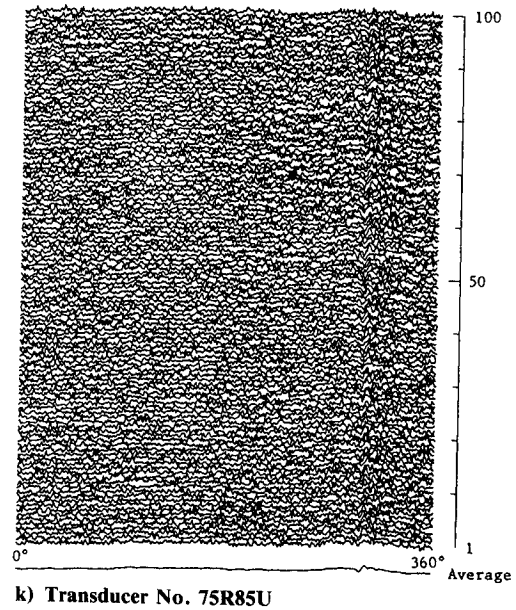

k) Transducer No. 75R85U

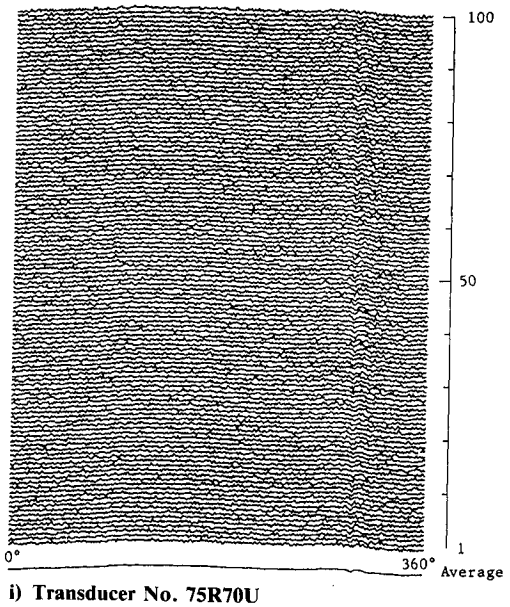

i) Transducer No. 75R70U

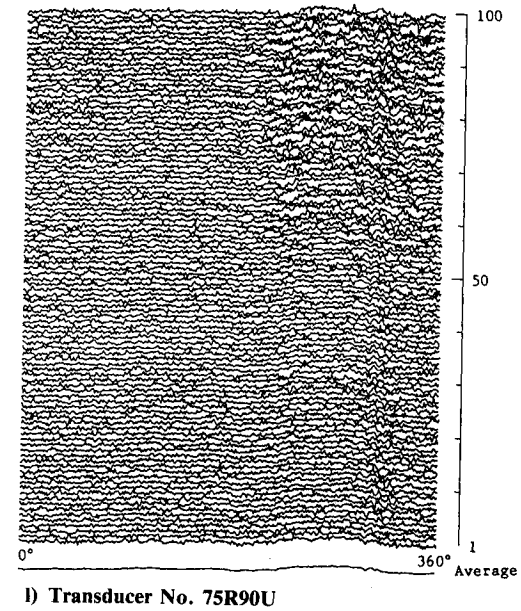

l) Transducer No. 75R90U

Fig. 5 (Continued) Pressure-time history over 100 revolutions at 75% propeller radius at flight condition 11; helical Mach number at 0.75R, $M_r = 0.585$, advance ratio $J = 1.13$, $\beta_{75R} = 25.7$ deg, and $\beta_{\text{prop}} = 26.6$ deg.

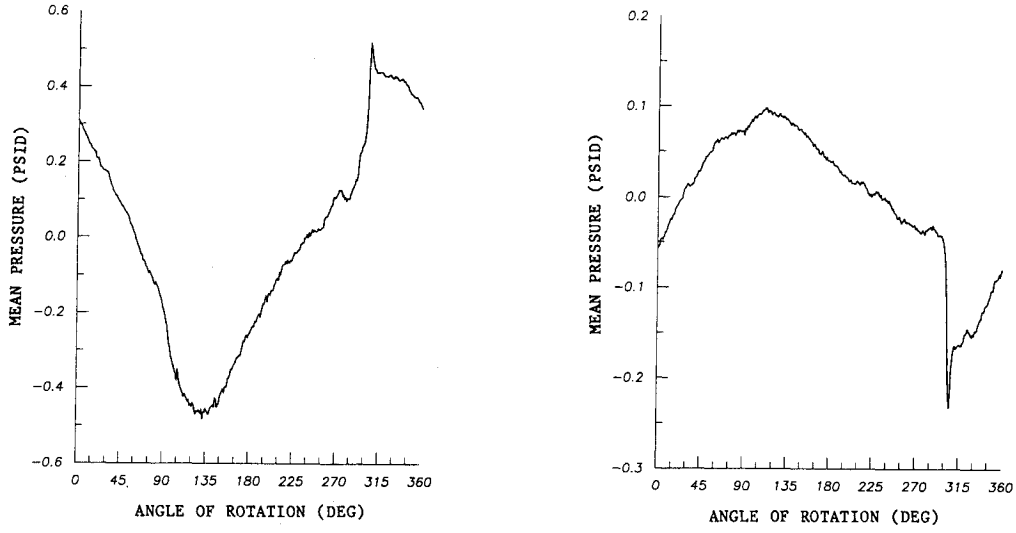

a) Transducer No. 75R05L

b) Transducer No. 75R05U

Fig. 6 Average pressure waveforms (over 100 revolutions) of 5% pressure and suction surface BMTs in flight condition 11 at 0.75 propeller radius; helical Mach number is 0.585.

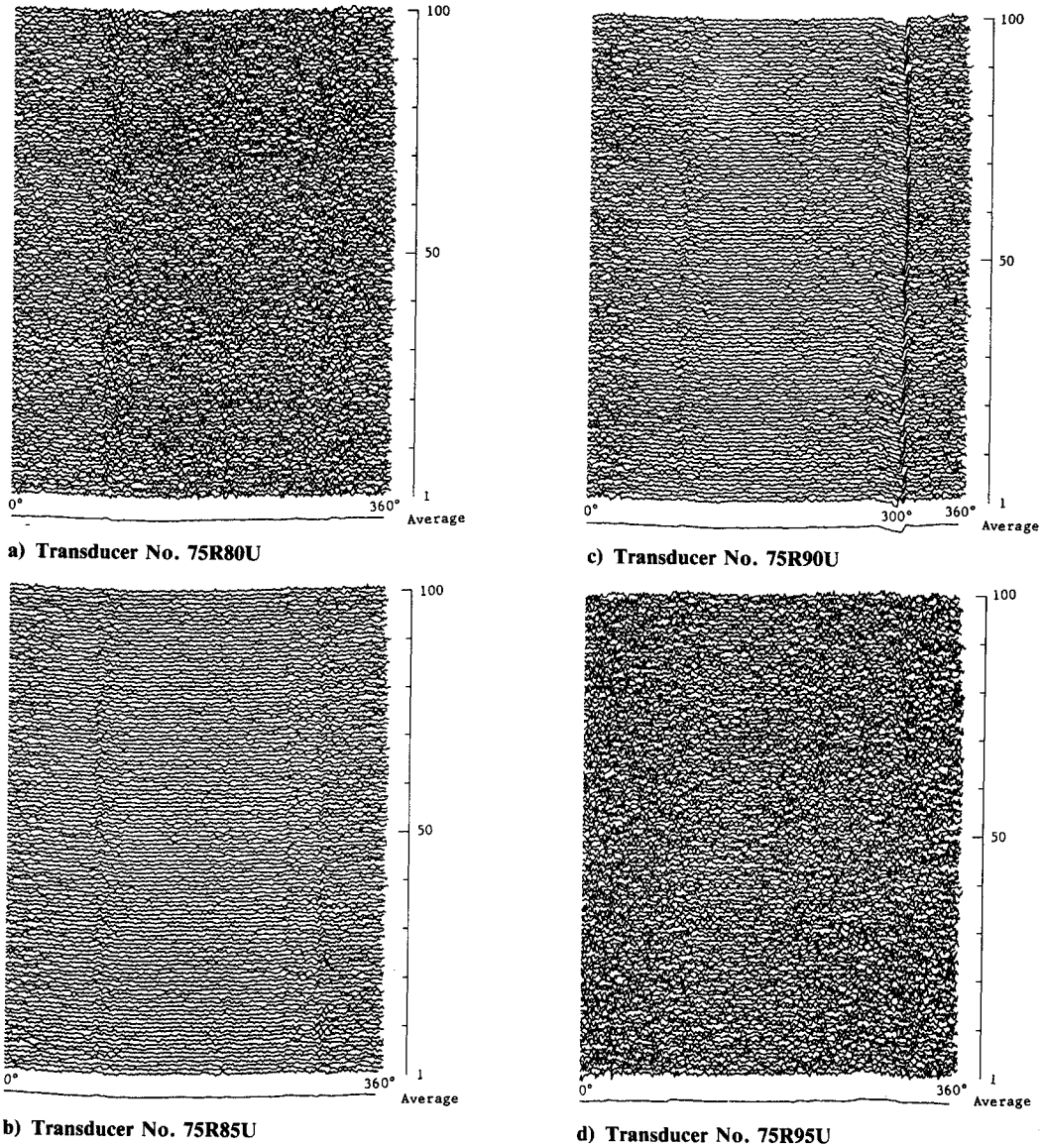

a) Transducer No. 75R80U

c) Transducer No. 75R90U

b) Transducer No. 75R85U

d) Transducer No. 75R95U

Fig. 7 Pressure-time history over 100 revolutions at 75% propeller radius at flight condition 2; helical Mach number $M_r = 0.687$, advance ratio $J = 1.47$, $\beta_{75R} = 32$ deg, and $\beta_{prop} = 36.3$ deg.

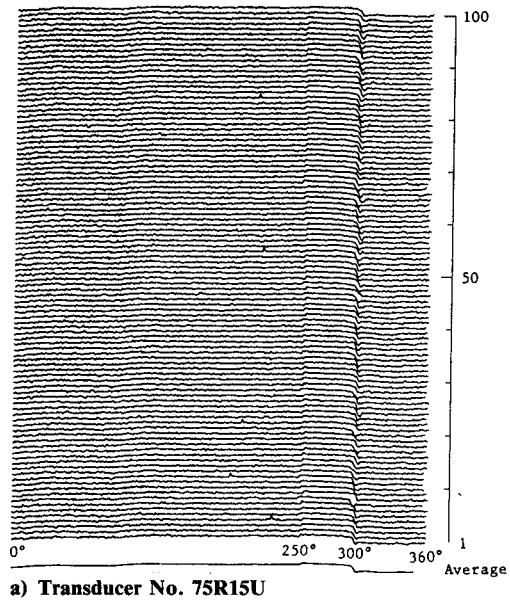

a) Transducer No. 75R15U

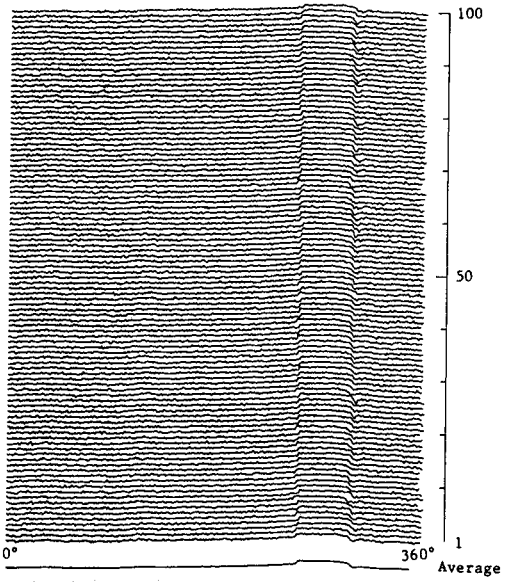

b) Transducer No. 75R20U

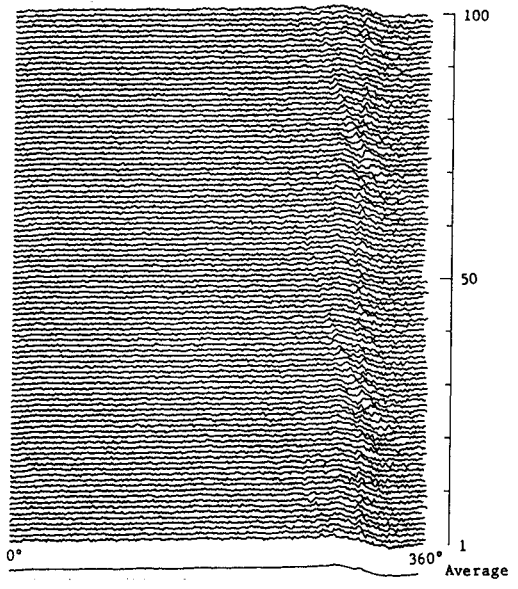

c) Transducer No. 75R60U

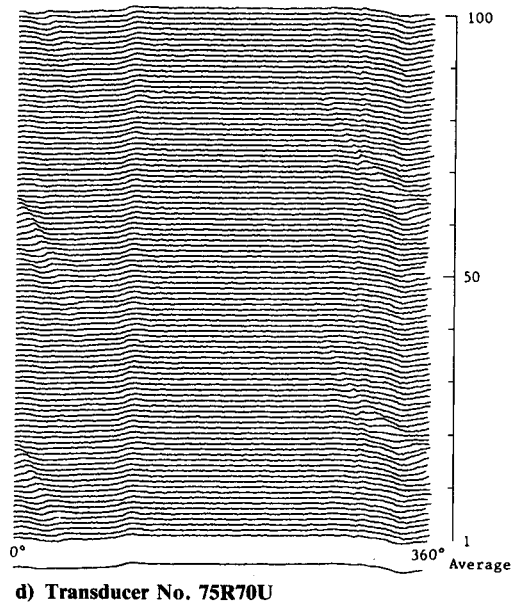

d) Transducer No. 75R70U

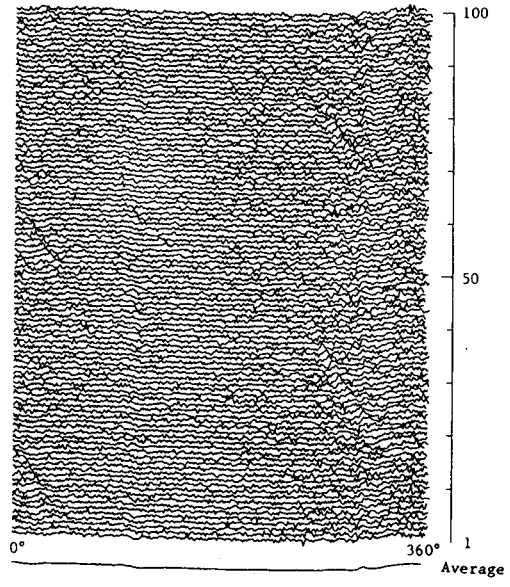

e) Transducer No. 75R80U

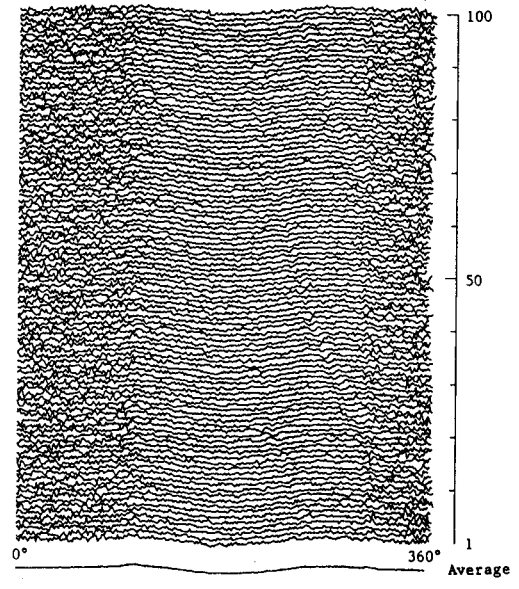

f) Transducer No. 75R90U

Fig. 8 Pressure-time history over 100 revolutions in flight condition 5; helical Mach number $M_r = 0.732$, advance ratio $J = 1.54$, $\beta_{75R} = 33.2$ deg, and $\beta_{prop} = 34.1$ deg.

(mean) loading, may be thought of as rather expected. At higher helical Mach numbers and loadings, upstream wake encounter will induce Mach waves and shock formation, which can completely change the nature of the expected wake signature.

In flight condition 2, with zero flap deflection, the 75% propeller radius operates at relative Mach number $M_r = 0.687$, propeller advance ratio $J = 1.47$, and mean loading $\Delta\beta = 4.3$ deg. The pylon wake minimum velocity introduces the 75% propeller section to $\Delta\beta_{max} = 12.4$ deg. Figure 7a shows a random turbulence signature at 80% chord BMT. At 85% transducer location, i.e., Fig. 7b, turbulent pressure fluctuations have somewhat subsided, and stationary waves in the propeller plane are observed. No pylon coherent wake signature on the propeller may be discerned from Figs. 7a and 7b. However, in Fig. 7c the 90%-chord BMT registers a turbulent pressure-time history that clearly identifies the wake signature at a 300-deg propeller position. Now this behavior, i.e., the re-emergence of the wake signature further downstream, was unexpected. Can this be a shock at 90% chord in response to upstream wake passage? The answer is no, since the BMT traces show a negative pressure pulse corresponding to suction rather than compression wave at the 300-deg position. Nonlinear wave interactions in a compressible turbulent boundary layer with external forcing may hold the key to this intriguing phenomenon. Figure 7d, at 95% chord position, shows a random turbulence signature re-emerging near the trailing edge.

Flight condition 5, with zero flap deflection, is characterized by $M_r = 0.732$, $J = 1.54$, and $\Delta\beta = 0.9$ deg. The maximum flow angle during pylon wake encounter is $\Delta\beta_{max} = 8.7$ deg. Figure 8a shows the pressure-time history for a 15% suction surface transducer. The negative pressure pulse near the 300-deg position identifies the upstream wake signature. Near the 250-deg position, a stationary positive surface pressure rise is visible. This behavior may be associated with compression Mach waves, i.e., a weak shock resulting from the one-cycle flow angularity in the propeller plane. Slightly downstream, i.e., at the 20% chord BMT position, the compression wave is further strengthened due to coalescence of more compression

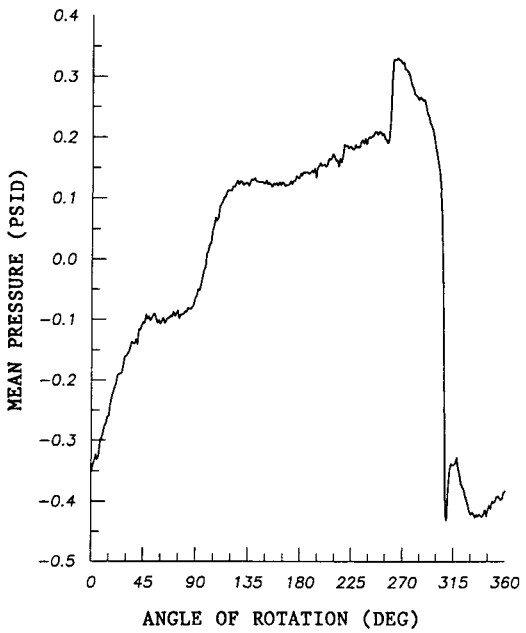

a) Transducer No. 75R15U Flight 1495 Cond. #5

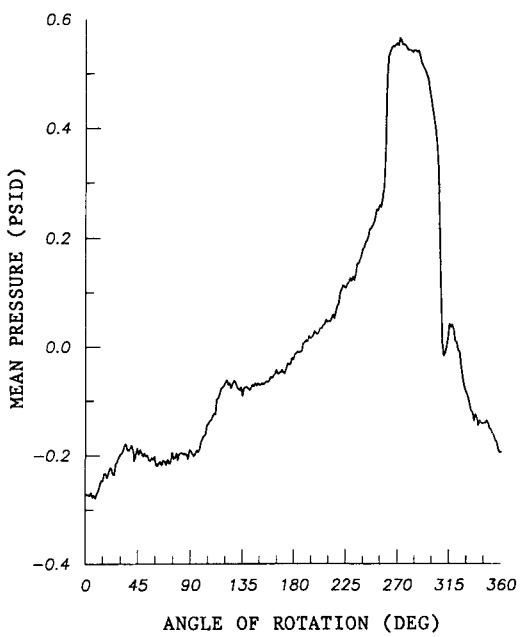

b) Transducer No. 75R20U Flight 1495 Cond. #5

Fig. 9 Average pressure waveforms over 100 revolutions in flight condition 5, for 15 and 20% transducers.

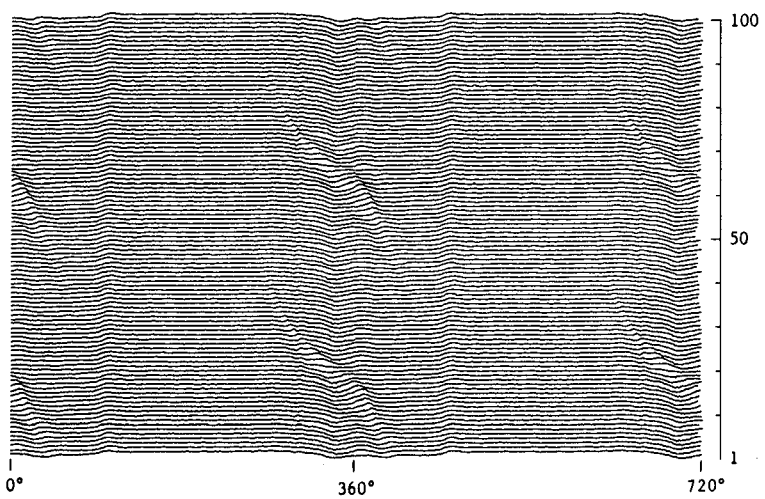

Fig. 10 Pressure-time history at 0.75R and 0.7 chord for flight condition 5; helical Mach number $M_r = 0.732$, propeller advance ratio $J = 1.54$, $\beta_{75R} = 33.2$ deg, and $\beta_{prop} = 34.1$ deg.

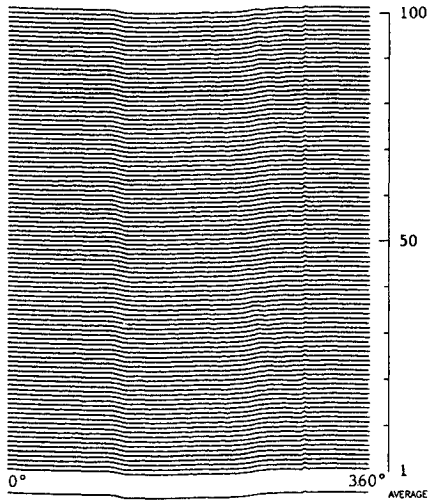

a) Transducer No. 90R10L Flight 1503 Cond. #3

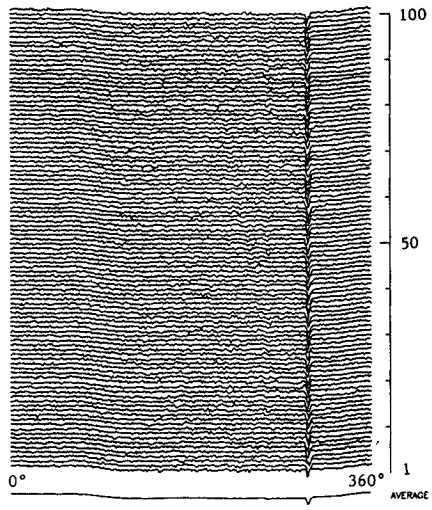

b) Transducer No. 90R20U Flight 1503 Cond. #3

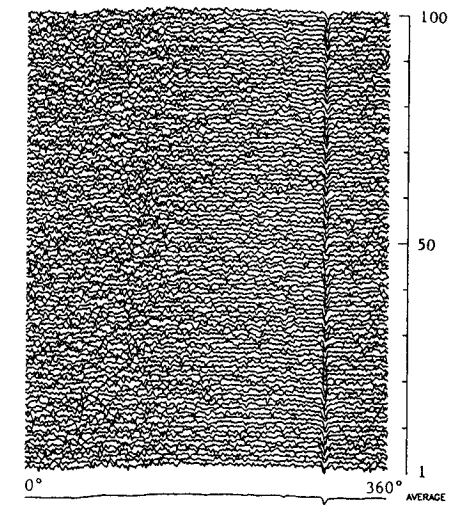

c) Transducer No. 90R40U Flight 1503 Cond. #3

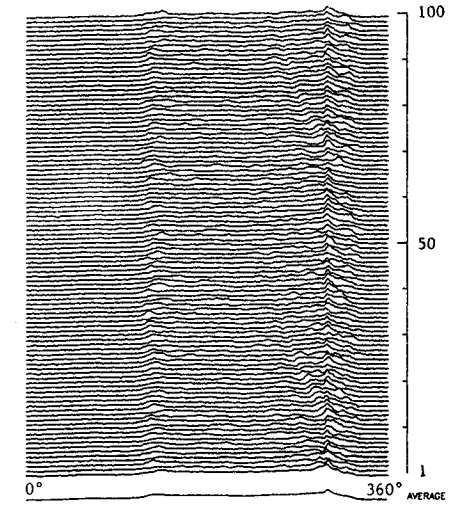

d) Transducer No. 90R80U Flight 1503 Cond. #3

Fig. 11 Pressure-time history at 0.9 propeller radius; helical Mach number $M_r = 0.935$, advance ratio $J = 1.53$, $\beta_{90R} = 28.5$ deg, and $\beta_{prop} = 30.3$ deg.

Mach waves, as shown in Fig. 8b. The average waveforms (over 100 revolutions) for these two transducers are shown, on a magnified scale, in Figs. 9a and 9b, respectively. The presence of a weak shock near 250 deg is clearly visible in Fig. 9. The axial distance between the 15 and 20% BMTs is 0.35 in. (8.9 mm), which may even correspond to the diffusion length scale in a lambda shock. At the 60% chord position, in this flight condition, a nonstationary new structure in the turbulent pressure history emerges, as shown in Fig. 8c. These slowly evolving "streaks" are periodic and persist downstream. Figures 8c–8f show the presence of the aforementioned periodic structures.

The slowly evolving, nonstationary, periodic surface events can best be seen in Fig. 10 in a double-cycle format. The cyclic period of these events is around 40 to 50 propeller revolutions, which in flight condition 5 is $T_{prop} \cong 30$ ms. Hence, the phenomenon repeats itself in every 1.2 to 1.5 s. This is three orders of magnitude longer than the chordwise convection time scale (based on the relative speed) of nearly 1 ms. It is interesting to note, as will be shown later, that similar blade surface pressure waves are discernible from the 0.8-chord BMT at the 90% propeller radius. Because of the long time scale of the periodic phenomenon, i.e., ~1 s, the possibility of the blade elastic mode natural frequencies matching the period of the measured disturbance is ruled out. However, the possibility of pylon-fuselage corner vortex impinging on the propeller tip as a result of aircraft roll oscillation is believed to exist.[3] This very intriguing phenomenon is currently under further investigation.

Positive flap deployment was exercised in flight conditions 13–26. It introduced a negative angle of attack to the pylon with the subsequent downward shift and widening of the pylon wake. Propeller interaction with upstream wake for these flight conditions, i.e., 12–26, will not be discussed here due to space limitation.

90% Propeller Radius

Eight blade-mounted pressure transducers were applied to the $0.9R$ propeller section. The BMT locations are at $x/c = 0.1$ pressure surface and $x/c = 0.1$, 0.2, 0.3, 0.4, 0.5, 0.60, and 0.80 suction surface positions.

In flight condition 3, with zero flap deflection, the helical Mach number at $0.9R$ was 0.935, propeller advance ratio $J = 1.53$, $\beta_{90R} = 28.5$ deg, and $\beta_{prop} = 30.2$ deg. Assuming that the pylon wake profile measured at a location corresponding to 75% propeller radius is also the deficit profile for

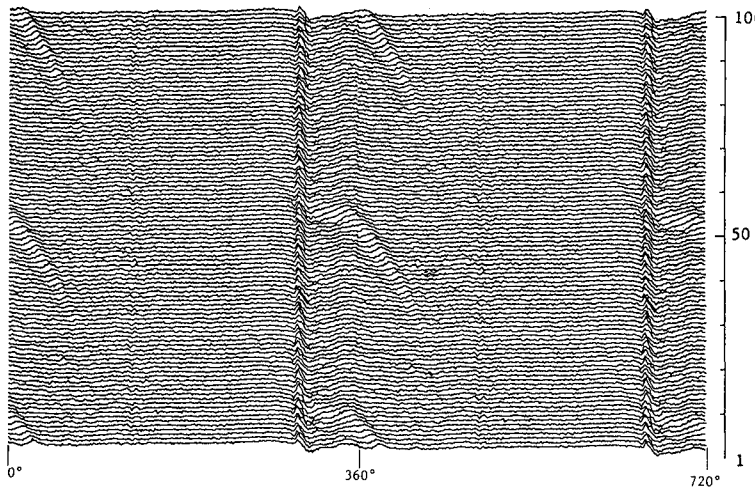

Fig. 12 Pressure-time history of 0.8*C*, 0.9*R* BMT, at flight condition 8; helical Mach number $M_r = 0.818$, propeller advance ratio $J = 1.30$, $\beta_{90R} = 24.8$ deg, and $\beta_{prop} = 22.1$ deg.

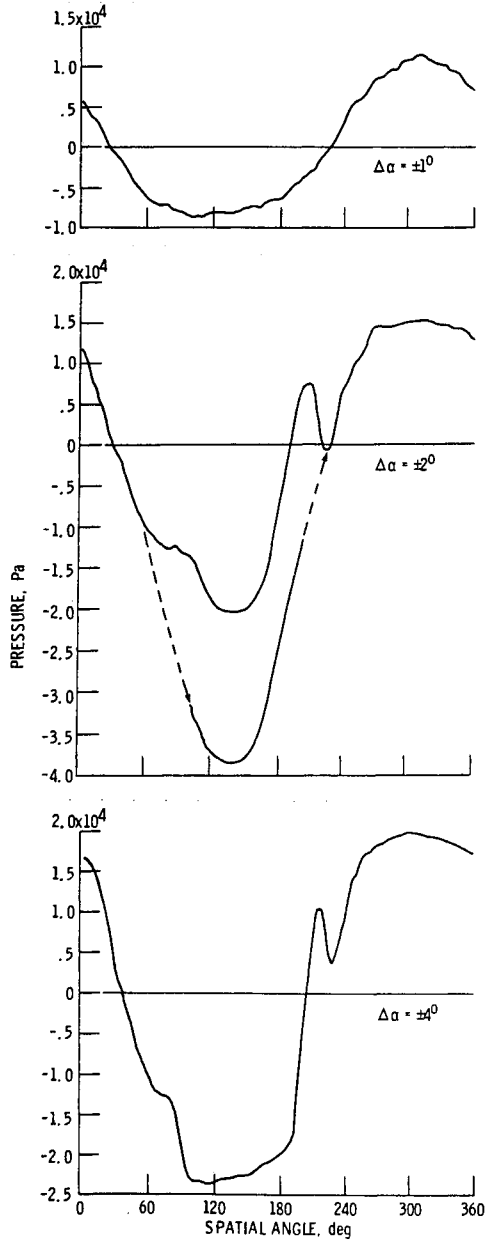

Fig. 13 Pressure waveforms for the suction surface at 0.75 radius and 0.1 chord, $M_\infty = 0.7$, $M_r = 0.885$, two blades.[4]

the 0.9*R*, the maximum $\Delta\beta$ encountered in the wake at this radius is $\Delta\beta_{max} = 9.7$ deg. The combination of high relative Mach number and large incidence variation in the wake encounter promotes shock formation on the suction surface. Figures 11a–11d show the pressure-time history of the four operational transducers in this flight condition. A very clear suction pulse at near the 300-deg azimuthal location is discernible from Figs. 11b and 11c. At 0.8*c*, the BMT location corresponding to Fig. 11d, three surface pressure events in response to azimuthal loading may be observed. First, stationary compression Mach waves around the propeller angular position of 120 deg are noted. This must be propeller response to one-cycle flow angularity due to angle of attack and/or sideslip. Second, we note the presence of a stationary shock at 0.8*c* due to wake encounter. The shock pressure imprint on the surface is seen as a positive pressure pulse at the 300-deg location. Finally, closer examination reveals a nonstationary, slowly evolving phenomenon of the type discussed earlier.

Pressure-time history of the 0.8-chord pressure transducer at 0.9*R* for flight condition 8 is shown (in double format, i.e., 0–720 deg) in Fig. 12. Again, the presence of a stationary compression wave is noted at the 300-deg position due to wake encounter. Nonstationary blade surface events of periodic nature and a long time scale are seen in Fig. 12 as well. It is interesting to note that these structures are observed in two different flights, i.e., flights 1497 and 1503.

To demonstrate the change of character of the blade-surface response to cyclic loadings of various amplitudes, the results of Heidelberg and Clark[4] are shown in Fig. 13. The experiment was conducted on advanced, highly swept SR-3 propeller blades in the NASA-Lewis 8 × 6 ft, supersonic wind tunnel. As the propeller blades were in tractor configuration, the angle of attack between the propeller shaft axis and V_∞ was the only source of periodic loading. Sinusoidal pressure response to small angle of attack ($\Delta\alpha = \pm 1$ deg), as shown in Fig. 13a, is typical of subsonic surface Mach number distributions on a lifting surface. However, the blade-surface response completely changes character at higher loadings, namely $\Delta\alpha = \pm 2$ or ± 4 deg. At these flow angularities and a helical Mach number of 0.885, shock-boundary-layer interaction distorts the sinusoidal surface pressure behavior considerably, as seen in Fig. 13. Candidate phenomena of boundary-layer separation and reattachment, i.e., separation bubble and shock oscillation, are suggested by Heidelberg and Clark[4] for the observed BMT response. The dashed line in Fig. 13b represents the reconstructed waveform by the authors eliminating sudden pressure changes in the BMT response.[4]

Farokhi and Vertzberger[5,6] have performed preliminary statistical data analysis on the flight data presented in this

paper, following Hanson.[7] Higher spectral analysis of the random data using the techniques outlined by Bendat and Piersol[8,9] are currently under way by Farokhi and will be reported shortly.

Concluding Remarks

Various interesting and peculiar aspects of pressure-time history on a pusher propeller blade in flight are presented and discussed. These range from a one-cycle flow angularity disturbance to shock-boundary-layer interactions due to upstream wake encounter. The three-dimensional turbulent boundary layer, in the transonic range, subject to periodic external forcing, is believed to hold the key to the observed peculiarities on the surface pressure traces. Considerable decay of turbulence fluctuations are noted from 0.8- to 0.9-chord BMT pressure-time histories in many flight conditions. A new type of periodic disturbance of long-time scale is discovered at positions beyond 0.6 chord on the suction surface in the transonic regime. This phenomenon is under further investigation. Further insight into the problem can be gained by spectral analysis of the recorded signals, which has been partially completed and is currently pursued. The effect of skew on the turbulent boundary-layer response to periodic loading in our studies may be investigated through propeller advance ratio J. This unconventional approach to the traditional role of propeller advance ratio is also under investigation. Finally, it is to be noted that pylon wake was measured at a station corresponding to a propeller with a 75% radius and was assumed to represent the deficit flow at the 90% propeller section as well. Also, the information on the pylon wake was not extrapolated to propeller face via wake diffusion formulas, e.g., Schlichting,[10] in this paper.

Acknowledgments

The research work presented in this paper is sponsored by NASA Langley Research Center under Grant NAG-1-867. D. Dunham and F. Farassat are the technical monitors. The author acknowledges the help of many students who performed various data reductions and graphics for this research, in particular Scott Collis and Kyle Wetzel. The efforts of Nancy Hanson of the Flight Research Laboratory at the University of Kansas in preparation of this manuscript are greatly appreciated.

References

[1]Knight, V. H., Jr., "In-Flight Jet Engine Noise Measurement System," *Proceedings of the ISA 27th International Instrumentation Symposium,* Indianapolis, IN, April 1981.

[2]Schoenster, J. A., "Fluctuating Pressure Measurements on the Fan Blades of a Turbofan Engine During Ground and Flight Tests," AIAA Paper 83-0679, April 1983.

[3]Farassat, F., private communication, July 1989.

[4]Heidelberg, L. J., and Clark, B. J., "Preliminary Results of Unsteady Blade Surface Pressure Measurements for the SR-3 Propeller," AIAA Paper 86-1893, 1986; see also NASA TM-87352, July 1986.

[5]Farokhi, S., and Vertzberger, M., "Blade Surface Pressure Measurement on a Pusher Propeller in Flight," Society of Automotive Engineers, Warrendale, PA, Paper 891040, April 1989.

[6]Farokhi, S., and Vertzberger, M., "Analysis of Unsteady Aerodynamic Data on a Pusher Propeller in Flight," University of Kansas, Lawrence, KS, Flight Research Rept. KU-FRL-803-1, Dec. 1988.

[7] Hanson, D. B., "Study of Noise Sources in a Subsonic Fan Using Measured Blade Pressures and Acoustic Theory," NASA CR-2574, 1975.

[8]Bendat, J. S., and Piersol, A. G., *Random Data: Analysis and Measurement Procedures*, 2nd ed., Wiley-Interscience, New York, 1986.

[9]Bendat, J. S., and Piersol, A. G., *Engineering Applications of Correlation and Spectral Analysis,* Wiley-Interscience, New York, 1980.

[10]Schlichting, H., *Boundary-Layer Theory*, 7th ed., McGraw-Hill, New York, 1979, p. 741.